Method of radial velocities for the estimation of aircraft wake vortex parameters from data measured by coherent Doppler lidar

I.N. Smalikho,[1,*] V.A. Banakh,[1] F. Holzäpfel,[2] and S. Rahm[2]

[1]*V.E. Zuev Institute of Atmospheric Optics SB RAS, 1 Akademik Zuev Square, Tomsk 634055, Russia*
[2]*Institute of Atmospheric Physics, German Aerospace Center (DLR), Münchener Straße 20, Oberpfaffenhofen, Wessling 82234 Germany*
[*]*smalikho@iao.ru*

Abstract: The method of radial velocities (RV) is applied to estimate aircraft wake vortex parameters from measurements conducted with pulsed coherent Doppler lidar (PCDL). Operations of the Stream Line lidar and the 2-μm PCDL are simulated numerically to analyze the accuracy of the estimated wake vortex parameters with the RV method. The RV method is also used to estimate wake vortex trajectories and circulation from lidar measurements at Tomsk and Munich airports. The method of velocity envelopes and the RV method are compared employing data gathered with the 2-μm PCDL. The domain of applicability of the RV method is determined.

OCIS codes: (010.3640) Lidar; (280.3340) Laser Doppler velocimetry.

References and links

1. V. I. Babkin, A. S. Belotserkovskiy, L. I. Turchak, N. A. Baranov, A. I. Zamyatin, M. I. Kanevsky, V. V. Morozov, I. V. Pasekunov, and N. Y. Chizhov, *Wake Vortex Flight Safety Systems for Aircrafts* (Nauka, Moscow, 2008), pp. 1–373. [in Russian]
2. F. Holzäpfel, T. Gerz, M. Frech, A. Tafferner, F. Köpp, I. Smalikho, S. Rahm, K.-U. Hahn, and C. Schwarz, "'The Wake Vortex Prediction and Monitoring System WSVBS - Part I: Design," Air Traffic Control Quarterly **17**(4), 301–322 (2009).
3. S. W. Henderson, P. J. M. Suni, C. P. Hale, S. M. Hannon, J. R. Magee, D. L. Bruns, and E. H. Yuen, "Coherent laser radar at 2 μm using solid-state lasers," IEEE Trans. Geosci. Rem. Sens. **31**(1), 4–15 (1993).
4. S. M. Hannon and J. A. Thomson, "Aircraft wake vortex detection and measurement with pulsed solid-state coherent laser radar," J. Mod. Opt. **41**(11), 2175–2196 (1994).
5. F. Köpp, S. Rahm, and I. N. Smalikho, "Characterization of aircraft wake vortices by 2-μm pulsed Doppler lidar," J. Atmos. Ocean. Technol. **21**(2), 194–206 (2004).
6. V. A. Banakh and I. N. Smalikho, *Coherent Doppler Wind Lidars in a Turbulent Atmosphere* (Artech House, Boston & London, 2013), pp. 1–248.
7. S. Rahm and I. N. Smalikho, "Aircraft wake vortex measurement with airborne coherent Doppler lidar," J. Aircr. **45**(4), 1148–1155 (2008).
8. I. N. Smalikho, F. Köpp, and S. Rahm, "Measurement of atmospheric turbulence by 2-μm Doppler lidar," J. Atmos. Ocean. Technol. **22**(11), 1733–1747 (2005).
9. G. Pearson, F. Davies, and C. Collier, "An analysis of performance of the UFAM Pulsed Doppler lidar for the observing the boundary layer," J. Atmos. Ocean. Technol. **26**(2), 240–250 (2009).
10. is V. A. Banakh, I. N. Smalikho, A. V. Falits, B. D. Belan, M. Y. Arshinov, and P. N. Antokhin, "Joint radiosonde and doppler lidar measurements of wind in the atmospheric boundary layer," Atmos. Oceanic Opt. **28**(2), 185–191 (2015).
11. V. A. Banakh and I. N. Smalikho, "Aircraft wake vortex parameterization based on 1.5-μm Coherent Doppler lidar data", Proceedings of 27th International Laser Radar Conference, New York, July 5–10, 2015 (accepted).
12. V. A. Banakh, A. Brewer, E. L. Pichugina, and I. N. Smalikho, "Measurements of wind velocity and direction with coherent Doppler lidar in conditions of a weak echo signal," Atmos. Oceanic Opt. **23**(5), 381–388 (2010).
13. T. Gerz, F. Holzäpfel, and D. Darracq, "Commercial aircraft wake vortices," Prog. Aerosp. Sci. **38**(3), 181–208 (2002).
14. C.W. Schwarz, K.U. Hahn, and D. Fischenberg, "Wake encounter severity assessment based on validated aerodynamic interaction models", AIAA Paper 2010 – 7679.

#243360 Received 19 Jun 2015; accepted 3 Aug 2015; published 25 Aug 2015

15. D. C. Burnham and J. N. Hallock, "Chicago monostatic acoustic vortex sensing system" U.S. Department of Transportation. Report No. DOT-TSC-FAA-79–103. 1982. 206 pp.
16. F. Köpp, S. Rahm, I. Smakikho, A. Dolfi, J.-P. Cariou, and M. Harris, "Comparison of wake-vortex parameters measured by pulsed and continuous-wave lidars," J. Aircr. **42**(4), 916–923 (2005).
17. F. Holzäpfel and M. Steen, "Aircraft wake-vortex evolution in ground proximity: Analysis and parameterization," AIAA J. **45**(1), 218–227 (2007).
18. F. N. Holzäpfel, A. Stephan, T. Misaka, and S. Körner, "Wake vortex evolution during approach and landing with and without plate lines", AIAA Paper 2014–0925.
19. F. Holzäpfel, A. Stephan, T. Heel, and S. Körner, "Enhanced wake vortex decay in ground proximity triggered by plate lines," Aircr. Eng. Aerosp. Technol., (2015), doi:10.1108/AEAT-02-2015-0045 (in print).

1. Introduction

The rotating air motion arising behind an aircraft can be dangerous for other flying vehicles encountering its wake zone [1]. For safety of airplanes during takeoff and landing, it is important to have real-time information available about the position (with respect to the flight corridor) and intensity of wake vortices generated by other landing or taking-off aircraft [2]. Pulsed coherent Doppler lidars (PCDLs) constitute currently the best technical facilities for experimental studies of aircraft wake vortices. They can also be used for monitoring of the wake situation over an airfield in real time.

A 2-μm PCDL is used most widely for the investigation of aircraft wake vortices [3]. The wake vortex parameters (coordinates of wake vortex axes and wake vortex circulation) are estimated from raw lidar data by different methods, which are described, for example, in [4,5]. The methods and results of extensive lidar studies of aircraft wake vortices in the atmosphere are considered in Chapter 5 of monograph [6].

A necessary condition for lidar measurements of wake vortex parameters is a rather high spatiotemporal resolution of the raw data and a high signal-to-noise ratio, which can be provided by the 2-μm PCDL in the atmospheric boundary layer. In the free atmosphere, where the concentration of aerosol particles is very low either contrails may contribute the required aerosols or smoke generators are installed on the aircraft wings [7].

In comparison with the 2-μm PCDL (the main parameters of this lidar can be found in [8]), the energy of the probing pulse E_P of the 1.5-μm Stream Line PCDL developed by HALO Photonics [9] is 20 times lower [10]. Therefore, the signal-to-noise ratio (SNR) for the Stream Line lidar at the same concentration of aerosol particles in air is few tens (approximately 50) times lower than the SNR of the 2-μm PCDL. On the other hand, the pulse repetition frequency of the Stream Line lidar is 30 times higher than that of the 2-μm PCDL. This allows achieving the required measurement accuracy even at the low signal-to-noise ratio.

The high SNR and the relatively long duration of the probing pulse leading to the insignificant (~0.6 MHz) instrumental broadening of the Doppler spectrum for the 2-μm PCDL [8] allows to apply the method of velocity envelopes (VE method) for the estimation of wake vortex parameters from lidar data [6]. However, this method cannot be applied to the processing of data of the Stream Line lidar due to its low SNR. For the Stream Line lidar another method for the determination of wake vortex circulation and positions was proposed [11]. This method employs the array of radial velocities measured by the lidar in order to obtain the required wake vortex information. In what follows, this method is referred to as the method of radial velocities (RV method). In [11], the RV method was tested in field experiment involving a Boeing 737-800 aircraft. However, questions concerning the accuracy of this method and its applicability to other types of PCDL and aircraft remained open.

This paper presents a modified version of the RV method. Operations of the Stream Line lidar and the 2-μm PCDL are simulated numerically to analyze the accuracy of the estimation of wake vortex parameters with this method. Further, results of lidar field experiments on the study of wake vortex axis trajectories and evolution of the wake vortex circulation obtained

#243360 Received 19 Jun 2015; accepted 3 Aug 2015; published 25 Aug 2015

with the RV method are presented. Finally, the wake vortex parameters estimated with the VE and RV methods are compared employing the 2-μm PCDL.

2. Lidars and measurement strategy

Table 1 summarizes the main parameters of the lidars used in our wake experiments. According to the tabulated data, the probing pulse duration τ_P determined at the FWHM power level for the Stream Line lidar is 2.35 times lower than that for the 2-μm PCDL. The Stream Line lidar obviously allows to measure the radial velocity with significantly better spatial resolution along the optical axis than the 2-μm lidar [8]. Thus, for the rectangular time window [6] with the width T_W = 120 ns, the longitudinal dimension of the probing volume $\Delta z = (cT_W / 2) / \mathrm{erf}[T_W / (2\sigma_P)]$ (c is the speed of light, $\sigma_P = \tau_P / (2\sqrt{\ln 2})$ and $\mathrm{erf}(x)$ is the error function integral) [6] is Δz = 30 m for the Stream Line lidar and Δz = 65 m for the 2-μm lidar.

Table 1. Parameters of Lidar Experiments

	Stream Line PCDL	2-μm PCDL
Wavelength [λ]	1.5 μm	2.022 μm
Pulse energy [E_P]	100 μJ	2 mJ
Pulse repetition frequency [f_P]	15000 Hz	500 Hz
Pulse duration [τ_P]	170 ns	400 ns
Focal length [F]	300 m	1500 m
Distance to runway [R_r]	315 m	850 m
Azimuth angle [θ]	0°	37.5°
Scanning rate [ω_s]	2°/s	1.2°/c
Maximal elevation angle [φ_M]	15°	6°
Minimal range [R_0]	150 m	360 m
Pulse number [N_a]	1500	25
Duration of measurement [ΔT]	0.1 s	0.05 s
Angular resolution [$\Delta\varphi$]	0.2°	0.0545°
Time window [T_W]	120 ns	120 ns
Probing volume [Δz]	30 m	65 m

For wake vortex measurements with a ground-based PCDL, the probing beam scanning is used in a vertical plane intersecting the aircraft flight path. At every scan, the beam intersects the wake behind the aircraft, pointing into the cross section where the two vortices are circulating in opposite directions, until the wake vortex vanishes or leaves the scanning sector. Figure 1 shows the measurement geometry, where the PCDL is installed at a distance R_r from the runway measured along the Y axis perpendicular to the runway. The probing beam scanning at the angular rate ω_s (absolute value) within the prescribed limits of variation of the elevation angle $0° \le \varphi \le \varphi_M$ is carried out in the ZY' plane at the azimuth angle θ to the Y axis. A landing aircraft, while flying over the runway, intersects the scanning plane at the height Z_A at the time t_A.

#243360 Received 19 Jun 2015; accepted 3 Aug 2015; published 25 Aug 2015

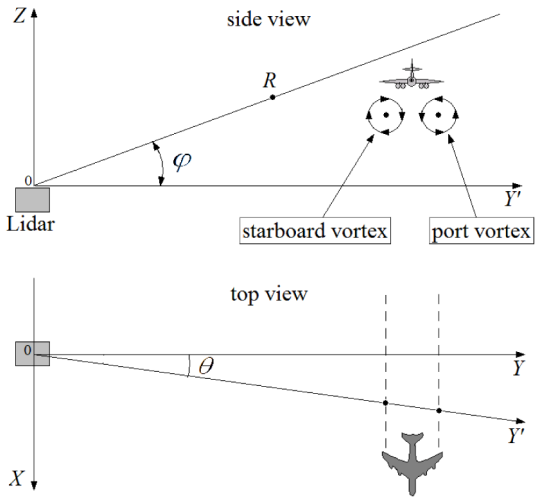

Fig. 1. Geometry of measurement by PCDL scanning in the vertical plane.

The raw data measured by the Stream Line lidar consists of the array of estimates of the correlation functions of the normalized complex lidar signal $\hat{C}(lT_s, R_k, \varphi_m; n')$, where $l = 0, 1, ..., 6$, $T_s = B^{-1}$ is the sampling interval, B = 50 MHz is the frequency bandwidth, $R_k = R_0 + k\Delta R$ is the distance from lidar, R_0 is the minimal measurement range, $k = 0, 1, ..., K-1$, $\Delta R = cT_s / 2$ = 3 m is the step in range, $\varphi_m = m\Delta\varphi$ is the elevation angle, $m = 0, 1, ..., M$, $\Delta\varphi = \omega_s \Delta T$ is the scanning angle resolution, $\Delta T = N_a / f_P$ is the duration of the measurement of the array $\hat{C}(lT_s, R_k, \varphi_m; n')$ at fixed m and n', N_a is the number of laser pulses used for accumulation of data [12], f_P is the pulse repetition frequency, and $n' = 1, 2, 3, ...$ is the scan number.

Let the lidar signal be normalized by the square root of the mean noise power. Then for the estimate of the signal-to-noise ratio $\mathrm{SNR}(R_k, \varphi_m; n')$ defined as a ratio of the mean power of the lidar echo signal to the mean noise power in the 50-MHz receiver passband, we have $\hat{\mathrm{SNR}}(R_k, \varphi_m; n') = \hat{C}(0, R_k, \varphi_m; n') - 1$. This estimate is unbiased, that is, $<\hat{\mathrm{SNR}}> = \mathrm{SNR}$, where the angular brackets denote ensemble averaging. In the measurements by the Stream Line lidar, the noise is not white. Therefore, first, the normalized correlation function of the noise component of the signal $C_N(lT_s)$ ($C_N(0)$ = 1) is determined from the raw data obtained from long distances R_k (in this case, the lidar measures only noise). Then, the equation $\hat{C}_S(lT_s, R_k, \varphi_m; n') = [\hat{C}(lT_s, R_k, \varphi_m; n') - C_N(lT_s)] / \hat{\mathrm{SNR}}(R_k, \varphi_m; n')$ is used to estimate the normalized correlation function of the useful component of the lidar signal $\hat{C}_S(lT_s, R_k, \varphi_m; n')$.

Using Eq. (5) from [12], we pass from $\hat{C}_S(lT_s, R_k, \varphi_m; n')$ to the array of estimates of Doppler spectra $\hat{S}_D(V_{l'}, R_k, \varphi_m; n')$, where $V_{l'} = (l' - L'/2)\delta V$, $l' = 0, 1, 2, ..., L'-1$, L' is the number of spectral channels, $\delta V = (\lambda / 2)B / L'$ is the velocity step, and λ is the wavelength. The number of spectral channels L' can be arbitrarily large (for example, L' = 1024). This is achieved by supplementing the array $\hat{C}_S(lT_s, R_k, \varphi_m; n')$ with the necessary number $L' - 7$ of complex zeros. As a rule, measurements by the Stream Line lidar are conducted at low SNR. This does not allow the spectral moments [4] and velocity envelopes [5] to be estimated from

#243360 Received 19 Jun 2015; accepted 3 Aug 2015; published 25 Aug 2015

the array $\hat{S}_D(V_{l'}, R_k, \varphi_m; n')$ with an acceptable accuracy. Therefore, to obtain the information about wake vortices from the Stream Line lidar data, we estimated the radial velocity $\hat{V}_r(R_k, \varphi_m; n')$ from the position of maximum of the Doppler spectrum, i.e. $\max\{\hat{S}_D(V_{l'}, R_k, \varphi_m; n')\} = \hat{S}_D(\hat{V}_r, R_k, \varphi_m; n')$.

The wake vortex parameters can be determined from the array $\hat{V}_r(R_k, \varphi_m; n')$ only if all estimates of radial velocities are unbiased. To meet this requirement it is necessary that the lidar echo signal and the number of accumulated pulses N_a are large enough. The focusing of the probing beam to some distance F allows a significant increase of the signal-to-noise ratio in the vicinity of the focus. The optimal parameters of experiment and data processing (F, R_r, θ, ω_s, φ_M, N_a, and T_W) for the Stream Line lidar were found in [11] and are summarized in Table 1. To compare the wake vortex trajectories and wake vortex circulation estimated by the RV and VE methods, we used the raw data of the 2-μm PCDL, whose parameters used during experiment and data processing are also summarized in Table 1. In the VE method, we specified the Gauss time window with the width T_W equal to the pulse duration τ_P. In this case, the probing length amounts to Δz = 90 m.

For the measurement geometry parameters of the Stream Line lidar from Table 1, the flight height Z_A should not exceed 60 m to enable the observation wake vortices immediately after their formation. The initial vortex separation b_0 is given by $b_0 = (\pi/4)B_A$, where B_A is the wing span [13]. At this measurement geometry, where the wake vortices interact with the ground surface already during vortex roll-up, the vortex separation always exceeds b_0. This is one of the conditions of applicability of the method of radial velocities.

3. RV method

Let the array of lidar estimates of the radial velocity $\hat{V}_r(R_k, \varphi_m; n')$ from the scan number $n' = n_0 + 1$ and to $n' = n_0 + N$ contain the information about wake vortices. To avoid the influence of the background wind, we obtain the data array

$$\tilde{V}_r(R_k, \varphi_m; n) = \hat{V}_r(R_k, \varphi_m; n_0 + n) - \hat{V}_r(R_k, \varphi_m; n_0), \tag{1}$$

where $n = n' - n_0 = 1, 2, ..., N$. A wake vortex influences most strongly lidar measurements of the radial velocity close to the vortex center starting from the distance r_C from the axis. The vortex core radius r_C is defined by the distance between the vortex center and the maximum tangential velocity and amounts to approximately 5% of the wing span B_A [14]. To estimate the coordinates of the port and starboard vortex axes from the array $\tilde{V}_r(R_k, \varphi_m; n)$, the functions $E(R_k; n)$, $\varphi_{\max}(R_k; n)$, and $\varphi_{\min}(R_k; n)$ were introduced in [11] as

$$\max_{\varphi}\{\tilde{V}_r(R_k, \varphi_m; n)\} = \tilde{V}_r(R_k, \varphi_{\max}; n), \tag{2}$$

$$\min_{\varphi}\{\tilde{V}_r(R_k, \varphi_m; n)\} = \tilde{V}_r(R_k, \varphi_{\min}; n), \tag{3}$$

$$E(R_k; n) = [\tilde{V}_r(R_k, \varphi_{\max}; n)]^2 + [\tilde{V}_r(R_k, \varphi_{\min}; n)]^2, \tag{4}$$

where maxima and minima of $\tilde{V}_r$ are sought for at every scan within the range of angles φ_m for different distances R_k. For every n, the functions $E(R_k; n)$ have two local maxima, whose positions give estimates of the distances from the lidar to the axes of the port vortex

#243360 Received 19 Jun 2015; accepted 3 Aug 2015; published 25 Aug 2015

($\hat{R}_{C1}(n)$) and starboard vortex ($\hat{R}_{C2}(n)$). The detailed description of the procedure how to find the maxima and how to identify the port and starboard vortices can be found in [11].

The angular coordinates of the axes of the port vortex ($\hat{\varphi}_{C1}(n)$) and starboard vortex ($\hat{\varphi}_{C2}(n)$) are estimated as

$$\hat{\varphi}_{Ci}(n) = [\varphi_{\max}(R_{Ci};n) + \varphi_{\min}(R_{Ci};n)]/2, \tag{5}$$

where the subscript i takes the values 1 and 2, respectively, for the port vortex and starboard vortex. The values of $\varphi_{\max}(R_{Ci};n)$ and $\varphi_{\min}(R_{Ci};n)$ in Eq. (5) are calculated by Eqs. (2) and (3) after application of the smoothing procedure (for example, moving average smoothing by seven points along the beam and three points across the beam) to the array $\tilde{V}_r(R_k,\varphi_m;n)$. To increase the accuracy of estimation of the vortex axis coordinates $\hat{R}_{Ci}(n)$, in this paper we replace $E(R_k;n)$ by the function

$$D(R_k;n) = \sum_m [\tilde{V}_r(R_k,\varphi_m;n)]^2. \tag{6}$$

The elevation angle $\varphi_m^{(n)}$ corresponding to the n-th scan is a function of time t measured from the instant as an aircraft intersects the scanning plane: $\varphi_m^{(n)} \equiv \varphi(t)$. The time $t_n^{(i)}$ of intersection of the axis of the i-th vortex by the probing beam for the n-th scan can be determined from the equality $\varphi(t_n^{(i)}) = \varphi_{Ci}(n)$. Using the obtained arrays $\hat{R}_{Ci}(n)$ and $\hat{\varphi}_{Ci}(n)$, we can represent the coordinates of vortex axis as functions of time in the Cartesian coordinate system:

$$\mathbf{r}_{Ci}(t_n^{(i)}) = \{Z_{Ci}(t_n^{(i)}) = \hat{R}_{Ci}(n)\sin[\hat{\varphi}_{Ci}(n)],\ Y_{Ci}(t_n^{(i)}) = \hat{R}_{Ci}(n)\cos[\hat{\varphi}_{Ci}(n)]\}. \tag{7}$$

The circulations of the port vortex $\hat{\Gamma}_1(t_n^{(1)})$ and starboard vortex $\hat{\Gamma}_2(t_n^{(2)})$ can be estimated by fitting of the array of velocities $\tilde{V}_r$ measured at the distances $\hat{R}_{Ci}$ to the theoretically calculated values as a result of the least-square minimization of the functionals $\rho(\Gamma_1)$ and $\rho(\Gamma_2)$:

$$\min\{\rho(\Gamma_i)\} = \rho(\hat{\Gamma}_i). \tag{8}$$

In Eq. (8),

$$\rho(\Gamma_i) = \sum_m [\tilde{V}_r(\hat{R}_{Ci},\varphi_m;n) - \bar{V}_r(\hat{R}_{Ci},\varphi_m \mid \Gamma_1,\Gamma_2)]^2, \tag{9}$$

where $\bar{V}_r(\hat{R}_{Ci},\varphi_m \mid \Gamma_1,\Gamma_2)$ is the radial velocity calculated theoretically at arbitrary values of vortex circulations Γ_1 and Γ_2. Since the radial velocity was estimated from the position of the maximum of estimates of the Doppler spectrum, we failed to find the analytical equation for the fitting function $\bar{V}_r(\hat{R}_{Ci},\varphi_m \mid \Gamma_1,\Gamma_2)$, and it was calculated numerically.

The algorithm for calculation of $\bar{V}_r(\hat{R}_{Ci},\varphi_m \mid \Gamma_1,\Gamma_2)$ [11] is based on the theory developed in [6] and can be reduced to the following. It can be shown that the normalized correlation function of the useful component of the complex lidar signal $C_S(lT_s,\hat{R}_{Ci},\varphi_m) = <\hat{C}_S(lT_s,\hat{R}_{Ci},\varphi_m)>$ for the Gaussian temporal profile of the probing pulse can be represented in the form

#243360 Received 19 Jun 2015; accepted 3 Aug 2015; published 25 Aug 2015

$$C_S(lT_s, \hat{R}_{Ci}, \varphi_m) = \int_{-\infty}^{+\infty} dz' A(l, z') \exp[2\pi j l B_V^{-1} V_r(\hat{R}_{Ci} + z', \varphi_m)], \quad (10)$$

where $A(l, z') = \frac{1}{7-l} \sum_{m'=0}^{6-l} Q(z' - (m'-3)\Delta R) Q(z' - (m'+l-3)\Delta R)$, $Q(z') = (\sqrt{\pi}\Delta p)^{-1/2} \exp[-(z'/\Delta p)^2/2]$, $\Delta p = c\sigma_P / 2$, $j = \sqrt{-1}$, $B_V = \lambda / (2T_s)$, and $V_r(R, \varphi)$ is the model function for the radial velocity. The function $V_r(R, \varphi)$ for the Burnham—Hallock vortex model [15] is described by the equation

$$V_r(R, \varphi) = \frac{1}{2\pi} \sum_{i=1}^{2} \frac{(-1)^i \Gamma_i \hat{R}_{Ci} \sin(\varphi - \hat{\varphi}_{Ci}) \cos\theta}{(R\sin\varphi - \hat{R}_{Ci}\sin\hat{\varphi}_{Ci})^2 + (R\cos\varphi - \hat{R}_{Ci}\cos\hat{\varphi}_{Ci})^2 \cos^2\theta + r_C^2}, \quad (11)$$

which results from Eqs. (5.1) and (5.6) from [6]. The correlation function $C_S(lT_s, \hat{R}_{Ci}, \varphi_m)$ calculated with Eq. (11) for different values of Γ_1 and Γ_2 is used to find the Doppler spectra $S_D(V_{l'}, \hat{R}_{Ci}, \varphi_m)$. Then the equations

$$\max\{S_D(V_{l'}, \hat{R}_{Ci}, \varphi_m)\} = S_D(\bar{V}_r, \hat{R}_{Ci}, \varphi_m), \quad (12)$$

are used to determine $\bar{V}_r(\hat{R}_{Ci}, \varphi_m \mid \Gamma_1, \Gamma_2)$.

The following iteration procedure is applied to obtain estimates $\hat{\Gamma}_1$ and $\hat{\Gamma}_2$. When the separation between the vortex axes becomes several times larger than the initial separation b_0, the vortices are practically independent. In this case, it is reasonable to take $\bar{V}_r = \bar{V}_r(\hat{R}_{C1}, \varphi_m \mid \Gamma_1, 0)$ and $\bar{V}_r = \bar{V}_r(\hat{R}_{C2}, \varphi_m \mid 0, \Gamma_2)$ in Eq. (9) for $\rho(\Gamma_1)$ and $\rho(\Gamma_2)$, respectively. After minimization of these functionals (Eq. (8)), we have estimates of circulation $\hat{\Gamma}_1^{(1)}$ and $\hat{\Gamma}_2^{(1)}$ in the first iteration. At the second iteration, $\bar{V}_r = \bar{V}_r(\hat{R}_{C1}, \varphi_m \mid \Gamma_1, \hat{\Gamma}_2^{(1)})$ and $\bar{V}_r = \bar{V}_r(\hat{R}_{C2}, \varphi_m \mid \hat{\Gamma}_1^{(1)}, \Gamma_2)$ are specified in Eq. (9) for $\rho(\Gamma_1)$ and $\rho(\Gamma_2)$, respectively. After minimization of $\rho(\Gamma_1)$ and $\rho(\Gamma_2)$, we obtain estimates $\hat{\Gamma}_1^{(2)}$ and $\hat{\Gamma}_2^{(2)}$. And so on. The numerical and field experiments have shown that this iteration algorithm converges rapidly. Three iterations are usually enough.

4. Numerical simulation results

The true coordinates and circulation of the i-th vortex specified are denoted as $R_{Ci}^{(T)}$, $\varphi_{Ci}^{(T)}$, and $\Gamma_{Ci}^{(T)}$ in the numerical simulation. To study the regular error in estimation of the distance from the Stream Line lidar to the axes of vortices generated by different aircraft types, we calculated the function $D(R_k)$ by Eq. (6) where $\tilde{V}_r$ was replaced by $\bar{V}_r$. The velocity $\bar{V}_r$ was calculated with Eqs. (10)-(12), where $\hat{R}_{Ci}$ was replaced by R_k. It was assumed that the circulations of the port vortex and starboard vortex are identical ($\Gamma_1^{(T)} = \Gamma_2^{(T)} = \Gamma$), the central point between the vortex axes is at the height Z_{center} = 30 m, and the line connecting the vortex axes is horizontal.

Figures 2(a, b) depicts $D(R_k)$ calculated for Γ = 150 m^2/s, b = 15 m, and r_C = 1 m (a) and Γ = 250 m^2/s, b = 27 m, and r_C = 1.7 m (b), where b is the separation between the vortex axes. For the calculations we used the parameters listed in Table 1 for the Stream Line lidar. Dashed lines show the prescribed positions of the vortex axes $R_{C1}^{(T)}$ and $R_{C2}^{(T)}$. It can be

#243360 Received 19 Jun 2015; accepted 3 Aug 2015; published 25 Aug 2015

seen from Fig. 2(a) that the positions of the maxima of $D(R_k)$ do not coincide with the dashed lines, that is, $\hat{R}_{C1} > R_{C1}^{(T)}$, while $\hat{R}_{C2} < R_{C2}^{(T)}$. This is explained by the averaging with the low-frequency spatial filter along the optical axis on the radial velocity (Eq. (11)).

When the longitudinal dimension of the probing volume of the Stream Line lidar Δz = 30 m exceeds the separation between the vortex axes b by far, the probing volumes centered at the axes of the port vortex and the starboard vortex overlap, and the RV method does not work sufficiently precise. In Fig. 2(b), $\Delta z \approx b$, the probing volumes do not overlap, and the maxima of $D(R_k)$ roughly coincide with the dashed lines. Our analysis shows that with the Stream Line lidar it is possible to estimate the wake vortex parameters with the acceptable accuracy during the initial vortex evolution, when $b \approx b_0 = (\pi/4)B_A$, for aircraft with a wing span $B_A \geq$ 30 m.

Figures 2(c, d) show $D(R_k)$ calculated for the 2-μm PCDL at Δz = 65 m. The calculations have been performed for Γ = 250 m^2/s, b = 27 m, r_C = 1.7 m (c) and Γ = 500 m^2/s, b = 63 m, r_C = 3.2 m (d); Z_{center} = 50 m and $\theta = 0°$. It can be seen that in Fig. 2(d) maxima $D(R_k)$ meet the dashed lines. Thus, acceptable estimates of wake vortex parameters can be obtained with the 2-μm lidar by the RV method only for big aircraft. Consideration of the azimuth angle of $\theta = 37.5°$ yields b = 63 m.

The accuracy of lidar estimates of wake vortex parameters was studied for the given vortex positions and circulations with the aid of closed numerical simulation. The algorithms described in [6] were used for computer simulation of random realizations of PCDL raw data, whose processing yielded arrays of radial velocities. The RV method was then applied to the resulting arrays of radial velocities. In the numerical experiments, the vortex coordinates $\{R_{Ci}^{(T)}, \varphi_{Ci}^{(T)}\}$ and the circulations $\Gamma_i^{(T)}$ of the port vortex (i = 1) and the starboard vortex (i = 2) were prescribed and, therefore, known exactly. This allowed us to calculate the errors of their estimation from the simulated lidar data by the equations $E_R = \sqrt{\frac{1}{2}\sum_{i=1}^{2} < \left[\hat{R}_{Ci} - R_{Ci}^{(T)}\right]^2 >}$, $E_\varphi = \sqrt{\frac{1}{2}\sum_{i=1}^{2} < \left[\hat{\varphi}_{Ci} - \varphi_{Ci}^{(T)}\right]^2 >}$, and $E_\Gamma = \sqrt{\frac{1}{2}\sum_{i=1}^{2} < \left[\hat{\Gamma}_i - \Gamma_i^{(T)}\right]^2 >}$ based on a statistically significant number of independent estimates of $\{\hat{R}_{Ci}, \hat{\varphi}_{Ci}\}$ and $\hat{\Gamma}_i$.

#243360 Received 19 Jun 2015; accepted 3 Aug 2015; published 25 Aug 2015

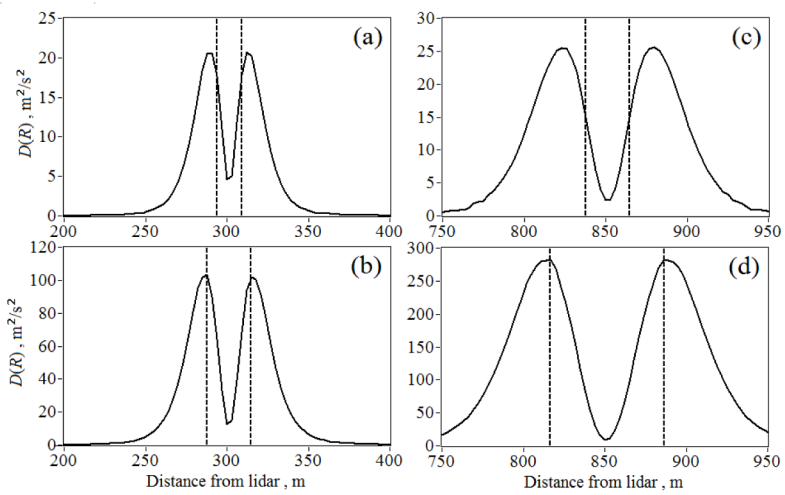

Fig. 2. Functions $D(R)$ for the Stream Line lidar (a, b) and the 2-μm PCDL (c, d) calculated at Γ = 150 m²/s, b = 15 m and r_C = 1 m (a); Γ = 250 m²/s, b = 27 m, and r_C = 1.7 m (b, c); Γ = 500 m²/s, b = 63 m, and r_C = 3.2 m (d). Dashed lines correspond to the preset model distances from the lidar to the axes of the port vortex and starboard vortex.

To calculate the errors E_R, E_φ, and E_Γ, it is necessary to specify the signal-to-noise ratio SNR in the numerical simulation. As follows from the experiments with the Stream Line lidar, at the measurement parameters presented in Table 1, SNR usually ranges from 0.05 to 0.25. Table 2 summarizes the theoretically calculated errors of lidar estimates of wake vortex parameters in this range of SNR. In the simulation, we assumed that the background wind was zero for the measurement parameters and wake vortex parameters corresponding to Fig. 2(b). The results obtained indicate the possibility of measuring the coordinates of axes of aircraft wake vortices and wake vortex circulation by the Stream Line lidar with the rather high accuracy.

Table 2. Theoretical Estimates of Errors in Determination of Wake Vortex Parameters from Data Measured by the Stream Line Lidar

SNR	0.05	0.1	0.2
E_R, m	1.8	1.5	1.3
E_φ, deg	0.21	0.13	0.1
E_Γ, m²/s	10.3	6.7	4.6

The closed numerical experiments employing the RV method have been carried out also for the parameters of the 2-μm PCDL in Table 1 and a typical (for this lidar) SNR = 10 at Γ = 500 m²/s, b = 50 m (63 m in scanning plane), and Z_{center} = 50 m. The calculated errors in this case were E_R = 5.6 m, E_φ = 0.16°, and E_Γ = 47.5 m²/s, which are higher than the corresponding errors in Table 2. That is, despite the significantly lower SNR values, the error of estimation of the radial velocity from the Stream Line lidar data appears to be less than the error of estimation of the radial velocity from the data of the 2-μm lidar because in the case of Stream Line lidar we use much more pulses for data accumulation (compare N_a in Table 1). The RV and VE methods for the 2-μm lidar yield comparable errors for the wake vortex axis coordinates, but for circulation the VE method gives a significantly lower error of E_Γ = 13 m²/s [16].

#243360 Received 19 Jun 2015; accepted 3 Aug 2015; published 25 Aug 2015

5. Field experiment results

During summer 2014 we have conducted a series of experiments at the airfield of the Tomsk Airport with the Stream Line lidar. The parameters of these experiments are given in the first column of Table 1. From all the obtained data, we selected only those, in which the probing beam was reflected by the aircraft at the time when the aircraft intersected the scanning plane. This allowed us to determine the vortex generation time t_A, the distance from the lidar to the aircraft, and the flight height Z_A with high accuracy.

Figure 3 shows results of lidar experiment conducted on 21 August 2014. Figure 3(a) shows the two-dimensional distribution of lidar estimates of the radial velocity $\tilde{V}_r(R_k, \varphi_m; 1)$ obtained from the first scan (n = 1). Figure 3(b) shows the distribution of the radial velocity along the optical axis of the probing beam propagating at the elevation angle φ_m = 4.2° one second after the intersection of the scanning plane by the aircraft. The velocity distribution in Fig. 3(b) corresponds to variation of the radial velocity along the cross section shown by the bold horizontal line in Fig. 3(a). The positions of the minimum and maximum of the radial velocity in this cross section are close to the axes of the starboard vortex and the port vortex, respectively. It is obvious that from the array of radial velocities shown in Fig. 3(a) it is impossible to estimate the aircraft wake vortex parameters, as the short time is not enough for the vortices to form completely.

Figure 3(c) shows the two-dimensional distribution $\tilde{V}(R_k, \varphi_m; 2)$ obtained for the following scan (n = 2), when the vortices are already further rolled up. The range of elevation angles φ_m, within which the summations in Eqs. (6) and (9) were performed, is indicated in Fig. 3(c). The function $D(R_k; 2)$ calculated from these data is shown in Fig. 3(d). The distance between the two maxima of this function is equal to 27 m, which coincides with the theoretical estimate of the initial separation between the vortex axes b_0 for a B737-800 aircraft, whose wing span is B_A = 34.32 m. The data shown in Fig. 3(c, d) were used to obtain the estimates $\hat{R}_{Ci}$, $\hat{\varphi}_{Ci}$, and $\hat{\Gamma}_{Ci}$ by the RV method. For the same case, Fig. 4 depicts the estimates of the Doppler spectra $\hat{S}_D(\tilde{V}_{l'}, \hat{R}_{Ci}, \varphi_m; n_0 + 2)$, where $\tilde{V}_{l'} = V_{l'} - \hat{V}_r(\hat{R}_{Ci}, \varphi_m; n_0)$. The results of calculation by Eq. (11) at $R = \hat{R}_{Ci}$ and r_C = 1.7 m are shown in this figure as blue curves. It can be seen that the calculated dependences of the radial velocity on the elevation angle correspond well with the Doppler spectra, thus indicating that the estimates of wake vortex parameters by the RV method are acceptable.

#243360 Received 19 Jun 2015; accepted 3 Aug 2015; published 25 Aug 2015

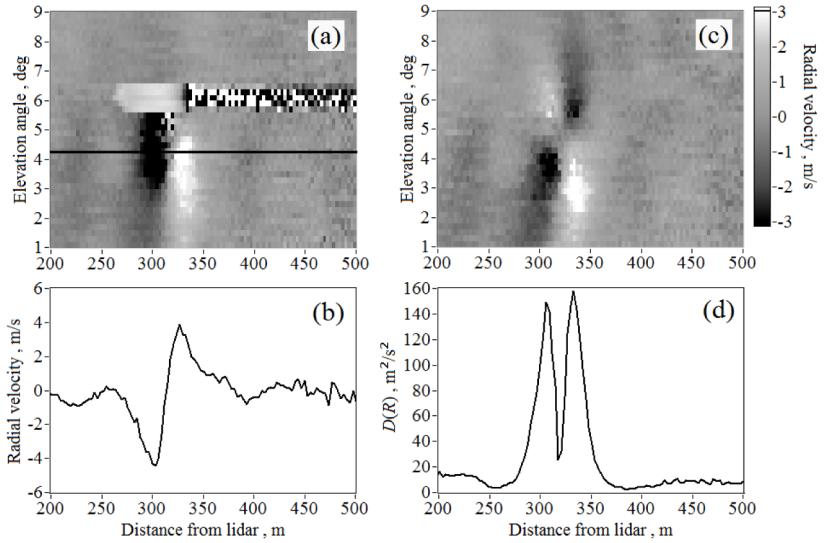

Fig. 3. Radial velocities $\tilde{V}_r(R_k,\varphi_m;1)$ (a), $\tilde{V}_r(R_k,\varphi;1)$ at φ = 4.2° (b), $\tilde{V}_r(R_k,\varphi_m;2)$ (c) and the function $D(R_k;2)$ (d) obtained from the measurements by the Stream Line lidar at the airfield of the Tomsk Airport on 21 August 2014. A landing B737-800 aircraft intersected the probing beam scanning plane at 07:45:24 LT at a height of 35 m.

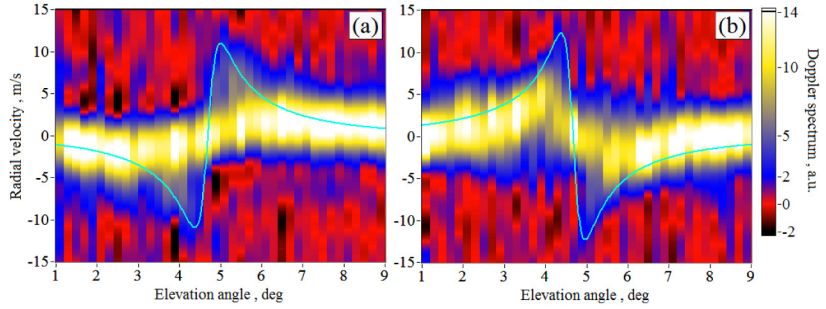

Fig. 4. Doppler spectra at different elevation angles φ_m and fixed distances $\hat{R}_{C2}$ (a) and $\hat{R}_{C1}$ (b). Blue curves are achieved by Eq. (11).

The evolution of vortex coordinates and circulations estimated from the lidar data by the RV method during the experiment with B737-800 on 21 August 2014 is shown in Fig. 5. It can be seen from Fig. 5(a) that in the initial period the vortices descend and simultaneously are transported laterally driven by the crosswind. The experimental estimate of the initial descend velocity $\hat{w} = [Z_A - Z_{Ci}(t_1^{(i)})]/t_1^{(i)}$ = 1.43 m/s is in good agreement with its theoretical estimate by the equation $w_0 = \Gamma_0/(2\pi b_0)$ = 1.47 m/s, where

$$\Gamma_0 = M_A g/(\rho_a b_0 V_A) \tag{13}$$

is the initial vortex circulation, g is the gravitational acceleration, ρ_a is the air density at the flight height, M_A is the aircraft mass, and V_A is the aircraft velocity [13]. Then the vortex descent terminates, and they are transported by the wind during the rebound of the port vortex. The background wind component within the scanning plane is estimated to 2.3 m/s which is close to the lateral drift velocity of the port vortex. Finally, at an age of 40 s the port

#243360 Received 19 Jun 2015; accepted 3 Aug 2015; published 25 Aug 2015

vortex reaches a height of whose axis 40 s later exceeding the height of the aircraft at the time when it intersected the scanning plane. In contrast to the port vortex, the starboard vortex descends down to a height of about 10 m, where it is lingering thereafter. The trajectories of vortex axes $\mathbf{r}_{Ci}(t_n^{(i)})$ shown in Fig. 5(a) are typical for aircraft wake vortex evolution in ground proximity, where the asymmetrical rebound is driven by the crosswind (see, for example, Chapter 5 in monograph [6] and paper [17]).

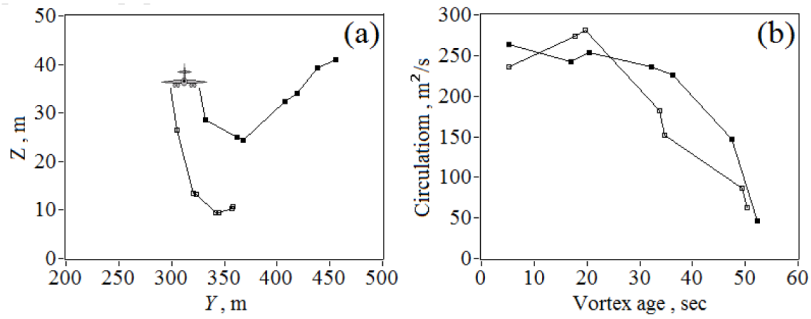

Fig. 5. Trajectories of vortex axes (a) and evolution of vortex circulation (b). The results are obtained by the RV method from the data measured by the Stream Line lidar at the airfield of the Tomsk Airport on 21 August 2014 once the B737-800 aircraft intersected the probing beam scanning plane at 07:45:24 LT.

Figure 5(b) illustrates the circulation evolution of the port vortex (closed squares) and the starboard vortex (open squares). For the B737-800 aircraft in the considered flight configuration the initial circulation calculated according to Eq. (13) yields Γ_0 = 250 m^2/s. One can see that the depicted estimates of the initial circulation (till 20 s) are close to the calculated Γ_0 within the error given in Table 2. With ongoing time the vortex intensity decreases, and the vortices practically vanish approximately 1 min after their formation.

To compare the RV and VE methods for the estimation of aircraft wake vortex parameters, the RV method was applied to raw data of the 2-μm lidar, which allows highly accurate estimations of the vortex parameters with the VE method [6]. Parameters of the lidar and the experiment conducted at the airfield of Munich Airport during 5 April 2011 are summarized in Table 1. Brief description of the Munich measurement campaign and statistical analyses of the 2-mm lidar wake vortex measurements are given in Refs [18, 19]. In order to fulfill the condition of applicability of the RV method for processing of 2-μm lidar data (see Section 3 of this paper), we have chosen the lidar data obtained with the A340-600 aircraft, for which, according to our calculations, b_0 = 50 m and Γ_0 = 500 m^2/s. Since in this experiment the azimuth angle is θ = 37.5°, the distance between the vortex axes in the probing beam scanning plane is $b_0 / \cos\theta$ = 63 m. Figure 6 exemplifies the array of the radial velocity $\tilde{V}_r(R_k, \varphi_m; 4)$ measured by the 2-μm lidar and the corresponding function $D(R_k; 4)$. The data presented are obtained for the fourth scan.

#243360 Received 19 Jun 2015; accepted 3 Aug 2015; published 25 Aug 2015

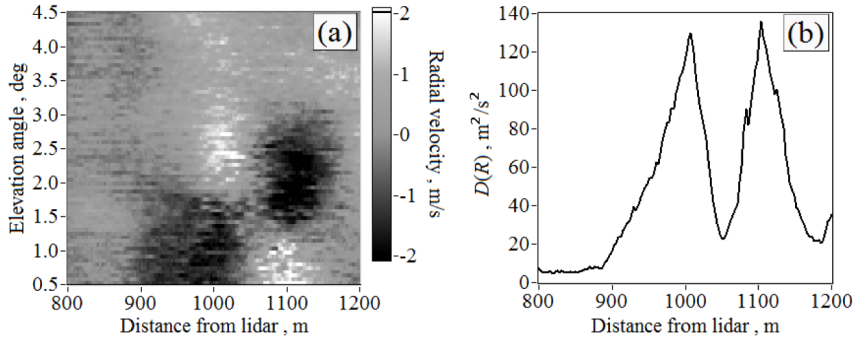

Fig. 6. Radial velocity $\tilde{V}_r(R_k, \varphi_m; 4)$ (a) and function $D(R_k; 4)$ (b) obtained from measurements with the 2-μm PCDL at the airfield of Munich Airport on 5 April 2011 once the landing A340-600 intersected the probing beam scanning plane at 07:28:05 LT.

The VE method [6] consists essentially in obtaining the positive and negative velocity envelopes from the measured Doppler spectra and estimating the aircraft wake vortex parameters from them. In contrast to the RV method, the VE method enables to obtain the results with acceptable accuracy for aircraft of any types under the condition of sufficiently high SNR . Figure 7 shows the results achieved by processing the data with the RV method (squares connected by solid lines) and with the VE method (circles connected by dashed lines) for a duration about 1 min after the A340-600 intersected the scanning plane. The closed squares (open circles) are for the port vortex, while open squares (closed circles) denote the starboard vortex. One can see that the methods yield rather similar results for vortex transport.

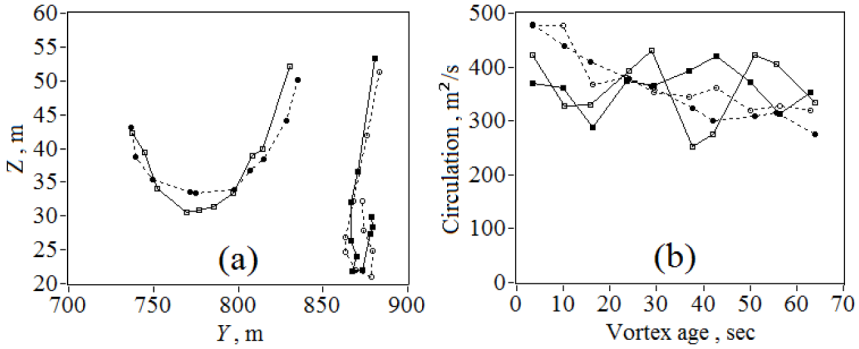

Fig. 7. Trajectories of vortex axes (a) and evolution of vortex circulation with time (b). The results are obtained by the RV method (squares connected by solid lines) and the VE method (circles connected by dashed lines) from the data measured by the 2-μm PCDL at the airfield of Munich Airport on 5 April 2011 once the A340-600 aircraft intersected the scanning plane at 07:28:05 LT.

The square roots of mean values of the square difference of the vortex parameters estimated by the RV and VE method are, by the data of Fig. 7, $\hat{E}_Z$ = 1.7 m for the vertical coordinate of the vortex axis, $\hat{E}_Y$ = 5.2 m for the horizontal coordinate of the vortex axis, and $\hat{E}_\Gamma$ = 70 m^2/s for the circulation. With allowance for the fact that the error of estimation of the circulation by the VE method is 13 m^2/s [16], the error of circulation estimation by the RV method is the major contributor to the error $\hat{E}_\Gamma$ = 70 m^2/s. The experimental error $\hat{E}_\Gamma$ is 1.5 times higher than the theoretical error of circulation estimation by the RV method E_Γ = 47.5

#243360 Received 19 Jun 2015; accepted 3 Aug 2015; published 25 Aug 2015

m^2/s from the data of the 2-μm lidar. This is possibly connected with the fact that in the numerical simulation we ignored inhomogeneity of the background wind, wind turbulence, and influence of the ground surface on the aircraft vortices.

6. Conclusions

In this paper, we discuss the applicability and accuracy of the method for estimation of aircraft wake vortex parameters from the array of radial velocities measured by the Stream Line lidar and 2-μm PCDL. It is shown that the RV method allows to estimate the position and circulation of aircraft wake vortices from raw data of the Stream Line lidar with an accuracy sufficient for the study of the spatial dynamics and evolution of wake vortices formed behind aircraft flying in the atmospheric surface layer. Owing to the comparatively long duration of the probing pulse, the RV method can be applied to measurement data of the 2-μm PCDL only for the estimation of wake vortex parameters of big aircraft. The error of the estimation of vortex position by the RV method in this case is comparable to the error of the VE method, while the relative error of the vortex circulation estimated by the RV method amounts to about 20%, which is 5 times higher than the relative error of the method of velocity envelopes. The RV method is applicable to data obtained under stationary conditions and weak wind turbulence, when the background wind velocity changes only slightly for the wake vortex lifetime.

Acknowledgments

This study was supported by the Russian Scientific Foundation for Maintenance and Development (Project 14-17-00386).

#243360 Received 19 Jun 2015; accepted 3 Aug 2015; published 25 Aug 2015